nature communications

Article

https://doi.org/10.1038/s41467-025-60429-6

Copper-catalyzed C(sp^3)–H amination and etherification of unactivated hydrocarbons via photoelectrochemical pathway

Received: 5 December 2024

Accepted: 19 May 2025

Published online: 02 June 2025

Check for updates

Jiawen Yin[1], Chengcheng Shi[1], Ao-Men Hu[1], Mengqi Luo[1], Chao Yang[1], Lin Guo[1] ✉ & Wujiong Xia[1,2] ✉

C(sp^3)–H activation and functionalization of unactivated hydrocarbons has provided enormous opportunities for the construction of diverse organic molecules, which facilitates the structural modification of pharmaceutical molecules. To achieve this goal, the direct hydrogen atom transfer (HAT) via radical pathway has become an attractive strategy. Taking the advantage of photo/electrochemistry, we herein describe oxidative C(sp^3)–H amination and etherification reactions via a photoelectrochemical pathway, which could directly transform easily available hydrocarbons into *N*-heterocycle and ether products under mild conditions. Applying 9-phenylacridine as a direct hydrogen atom transfer (d-HAT) reagent under 390 nm LED light irradiation and electrolysis, the scope of our method includes not only simple alkanes, but also a wide range of C(sp^3)–H molecules including ethers, thioethers, silanes, and amides. The reaction shows broad scope (>135 examples) and unconventional regioselectivity, with the occurrence of both C(sp^3)–H amination and etherification preferentially at the sterically unhindered positions. Furthermore, gram-scale experiments and relevant mechanistic investigations are carried out to illustrate the reaction mechanism.

Hydrocarbons are fundamental raw materials in physical science. The development of synthetic methodologies for the functionalization of simple and unactivated hydrocarbons has the potential to explore uncharted chemical space and construct complex molecular scaffolds[1–4]. Moreover, by directly activating aliphatic C–H bonds of hydrocarbons, chemists can bypass commonly used alkyl halides and organometallic reagents, and directly use the feedstock materials for late-stage derivatization of pharmaceutical molecules, natural products, agrochemicals and functionalized materials[5–8]. However, the strong bond dissociation energies (BDE: 96–101 kcal·mol^{-1}) of C(sp^3)–H bonds in alkanes, combined with their high redox potentials (usually above 3.0 V vs. SCE), have hampered the direct use of unactivated alkanes in synthetic transformations[9,10]. In recent years, photo-induced radical-mediated hydrogen atom transfer (HAT) strategy has been greatly expanded into this area, as the efficient conversion of visible light into chemical energy allows the direct functionalization of unactivated C(sp^3)–H bonds under thermodynamically unfavorable or kinetically inert conditions, overcoming the constraints of redox potentials under mild conditions[11,12]. Current hydrogen atom transfer methods that directly trap the generated carbon-centered radical intermediates include the use of diverse radical acceptors as well as transition-metal-catalyzed platforms, and a series of carbon-carbon and carbon-heteroatom bond forming reactions have been successfully achieved (Fig. 1a, transition metal = copper, iron, manganese, etc.)[13–17]. Among these developed protocols, C(sp^3)–H amination and etherification stand out as unique transformations, as the incorporation and manipulation of *N*-heterocycle, amine, and ether functionalities on hydrocarbons would provide a plethora of opportunities for the preparation of simple building blocks and drug intermediates[18]. Major challenges in current C(sp^3)–H amination protocols lie in the

[1]State Key Lab of Urban Water Resource and Environment, Harbin Institute of Technology (Shenzhen), Shenzhen, China. [2]School of Chemistry and Chemical Engineering, Henan Normal University, Xinxiang, Henan, China. ✉e-mail: guolin@hit.edu.cn; xiawj@hit.edu.cn

https://doi.org/10.1038/s41467-025-60429-6

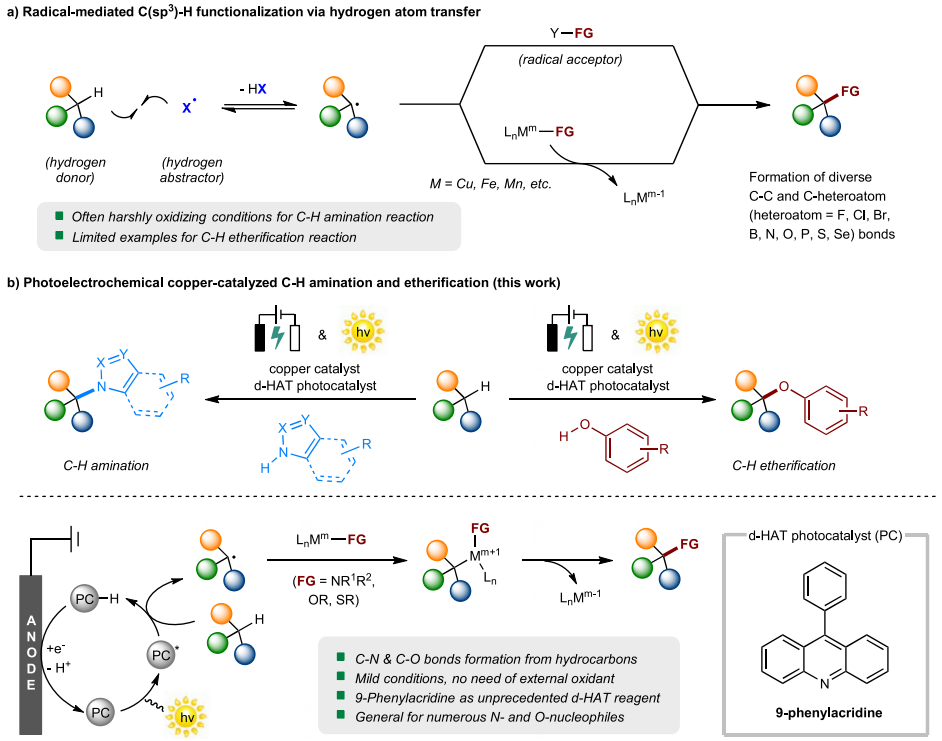

Fig. 1 | Prior art in radical-mediated C(sp^3)–H functionalization and an overview of this work. a Radical-mediated C(sp^3)–H functionalization via hydrogen atom transfer. **b** Photoelectrochemical copper-catalyzed C–H amination and etherification (this work).

limited substrate scope (e.g. occurence of amination only at benzylic C–H position)[19–29] as well as the requirement of stoichiometric oxidants and harsh reaction conditions[30–40]. On the other hand, C(sp^3)–H oxygenation reaction for the construction of ether products directly from simple alkanes has been rarely reported[41,42]. Therefore, exploration of catalysts and reagents that allow the selective functionalization of unactivated hydrocarbons under more practical and functional-group-tolerant conditions and with greater generality with respect to N- and O-coupling partners would be of great value.

With this in mind, we questioned whether our recent C(sp^3)–H functionalization work[43], combining HAT with a photoelectrochemical approach, would be suited to the development of a mild and general protocol for C(sp^3)–H amination and etherification. The use of electrons in electrochemistry as a green and economical redox reagent can overcome the high oxidation potential of alkanes in a milder and more practical way[44–47]. Simultaneous anodic oxidation and cathodic reduction reactions enable the transformation of a mild radical medium, eliminating the need for proton acceptor or stoichiometric oxidant/reductant[48–53]. In recent years, a series of photoelectrochemical strategies based on the advantages of photochemistry and electrochemistry have been reported, which further enrich the chemical conversion approaches[54–57]. The successful application of photoelectrochemical reactions with reference value provides a practical pathway for the direct C(sp^3)–H functionalization of unactivated hydrocarbons[58].

In this work, we present an efficient copper-catalyzed C(sp^3)–H amination and etherification protocol mediated by a photoelectrochemical hydrogen atom transfer process. Using easily available hydrocarbons as substrates, *N*-heterocycles and aromatic alcohols as coupling partners, this method enables the synthesis of the corresponding alkylated *N*-heterocycles and ethers in a single step (Fig. 1b). Key features of this study include: (1) the absence of external oxidant species, the use of inexpensive and readily available copper catalysts, ligands, electrolytes, additives, and solvents, along with mild reaction conditions, straightforward operation, scalability, and efficient performance in batch, highlighting the method's potential for industrial application; (2) a broad substrate scope, which has been expanded not only to diverse C(sp^3)–H hydrocarbons including simple alkanes, ethers, thioethers, silanes, amides, and aldehydes, but also to a series of N- and O-coupling partners; (3) most notably, the photoelectrochemical hydrogen atom transfer process is accomplished by the addition of 9-phenylacridine as a direct hydrogen atom transfer (d-HAT) reagent[11,12]. While the use of acridine salts as photocatalysts[59–64], electrophilic nitrogen-centered radicals (e.g., quinuclidine, amine, sulfonamide, amide, and azide) as d-HAT reagents has been widely reported[65,66], HAT reactions involving acridine-based *N*-centered radicals as cheap and easily available d-HAT reagents have not been explored yet[67–70]. Mechanistically, our reactions are proposed to proceed via photoexcitation of the d-HAT photocatalyst (PC) to generate PC* species, followed by hydrogen atom transfer with unactivated hydrocarbons, while electrochemical anodic oxidation promotes the transformation of PC-H back into PC species. Detailed mechanistic studies are further conducted to elucidate the reaction mechanism.

Results

Optimization studies

To explore the feasibility of the assembly of C(sp^3)–N bond on unactivated hydrocarbons, our studies were initiated by optimizing reaction conditions for the reaction of 3-bromo-1*H*-indazole (**1**) and cyclohexane (**2**), as shown in Table 1. The photoelectrocatalytic C(sp^3)–H amination reaction was conducted in an undivided cell (10 mL oven-dried quartz tube) equipped with a graphite rod anode and a platinum plate cathode. Upon electrolysis and 390 nm light irradiation, 9-phenylacridine was utilized as an efficient HAT catalyst under N_2 atmosphere. After an extensive evaluation of the reaction conditions, the corresponding aminated product (**3**) was afforded in 73% yield (Table 1, entry 1), employing $CuCl_2$ as catalyst, **L1** (3,4,7,8-tetramethyl-1,10-phenanthroline) as supporting ligand, Cs_2CO_3 as base, nBu$_4$NBF$_4$ as electrolyte in a mixed solvent of MeCN/DCM (2:1, *v*/*v*) under constant-current electrolysis at 3.0 mA for 6 h at room

https://doi.org/10.1038/s41467-025-60429-6

Table 1 | Optimization studies[a]

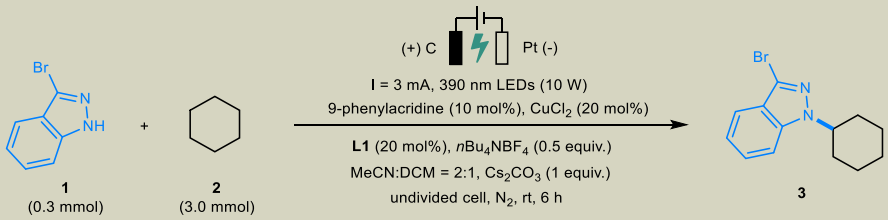

Entry	Variations from standard conditions	3 (%)[b]
1	None	73 (66[c])
2	$Cu(OTf)_2$ instead of $CuCl_2$	41
3	**L2** instead of **L1**	30
4	**L3** instead of **L1**	50
5	nBu_4NPF_6 instead of nBu_4NBF_4	35
6	BTMG instead of Cs_2CO_3	43
7	Using MeCN:DCE = 2:1 (*v*/*v*) as solvent	50
8	C(+)/C(−) instead of C(+)/Pt(−)	36
9	405 nm LEDs instead of 390 nm LEDs	23
10	Eosin Y or TBADT instead of 9-phenylacridine	N.D.
11	Without constant current	trace
12	Without $CuCl_2$ or Cs_2CO_3	N.D.
13	Without light irradiation or 9-phenylacridine	N.D.
14	Under air	46

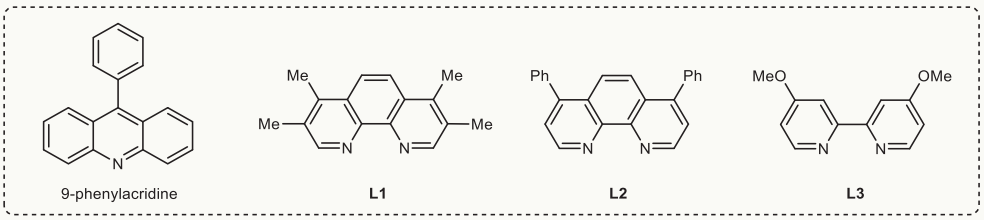

[a]Standard conditions: undivided cell, graphite rod anode (φ = 6 mm), platinum plate cathode (15 × 10 × 0.2 mm^3), 3-bromo-1*H*-indazole **1** (0.3 mmol, 1.0 equiv.), cyclohexane **2** (3.0 mmol, 10.0 equiv.), 9-phenylacridine (0.03 mmol, 10 mol%), $CuCl_2$ (0.06 mmol, 20 mol%), 3,4,7,8-tetramethyl-1,10-phenanthroline **L1** (0.06 mmol, 20 mol%), Cs_2CO_3 (0.3 mmol, 1.0 equiv.), nBu_4NBF_4 (0.15 mmol, 0.5 equiv., 0.05 M) and anhydrous MeCN:DCM = 2:1 (*v*/*v*, 3.0 mL), constant current = 3 mA, 390 nm LEDs (10 W) under N_2 atmosphere at room temperature for 6 h (2.2 $F \cdot mol^{-1}$).
[b]Unless otherwise stated, the yields were determined by GC-MS with *n*-tetradecane (0.3 mmol) as the internal standard.
[c]Yields of isolated products after chromatographic purification. *N.D.* not detected.

temperature. Notably, the use of other copper salts such as $Cu(OTf)_2$ led to decreased yield (entry 2). Supporting ligand plays a crucial role in the reaction, as the use of **L1** gave the best yield, whereas substituting **L1** with ligand **L2** (4,7-diphenyl-1,1-phenanthroline) or **L3** (4,4′-dimethoxy-2,2′-bipyridine) resulted in a substantial decrease in efficiency (entries 3-4). The experimental results showed that the replacement of nBu_4NBF_4 with nBu_4NPF_6 as electrolyte is unfavorable to the reaction (entry 5), and only a moderate yield was afforded using BTMG (2-*tert*-butyl-1,1,3,3-tetramethylguanidine) as base (entry 6). Moreover, the use of other solvents was explored but provided no improvement over mixed MeCN/DCM, and replacing the platinum plate cathode with a graphite rod cathode led to lower reaction efficiency (entries 7–8). In addition, the wavelength of the LEDs light source was also explored, but provided no improvement over 390 nm (entry 9). The use of Eosin Y or TBADT (tetrabutylammonium decatungstate) instead of 9-phenylacridine led to no reaction efficiency (entry 10). Control experiments indicated that electric current, catalysts, base and light irradiation are all essential, as the corresponding reactions performed without them resulted in poor or no reaction (entries 11-13). Further investigations revealed that the reaction was performed under air atmosphere with lower yield of the desired product (entry 14), indicating that the desired C(sp^3)–H amination product can be formed in the presence of oxygen, with loss of reaction efficiency.

Exploration of Substrate Scope

With the optimized reaction conditions in hand, we began to investigate the scope of *N*-heterocycles for this photoelectrochemical C(sp^3)–H amination reaction. As illustrated in Fig. 2, the *N*-alkylation reaction of indazoles with cyclohexane (**2**) was successfully demonstrated, yielding the corresponding products **3**–**12** in moderate to good yields. A range of indazole substrates bearing halide (**3**-**4**, **10**-**12**), aldehyde (**5**), nitrile (**6**), ester (**7**), ketone (**8**) and methyl moieties (**9**) proceeded well under the standard conditions. It is noteworthy that the photoelectrochemical reaction can be extended to substituted pyrazole (**13**–**18**), indole (**19**–**23**), pyrrole (**24**–**25**), carbazole (**26**–**27**), triazole (**28**–**29**), imidazole (**30**) and phthalazone (**31**), producing the corresponding amine products in moderate yields. Electron-rich *N*-heterocycles, such as 5-methoxyindole and 6-*tert*-butylindole, were found to be not suitable in our protocol. The substrate scope was then expanded to substituted anilines (**32**), aminopyridines (**33**–**37**), aminopyrimidine (**38**), and triazinamine (**39**), delivering the corresponding C(sp^3)–H amination products in moderate yields. Benzamides (**40**–**48**),

https://doi.org/10.1038/s41467-025-60429-6

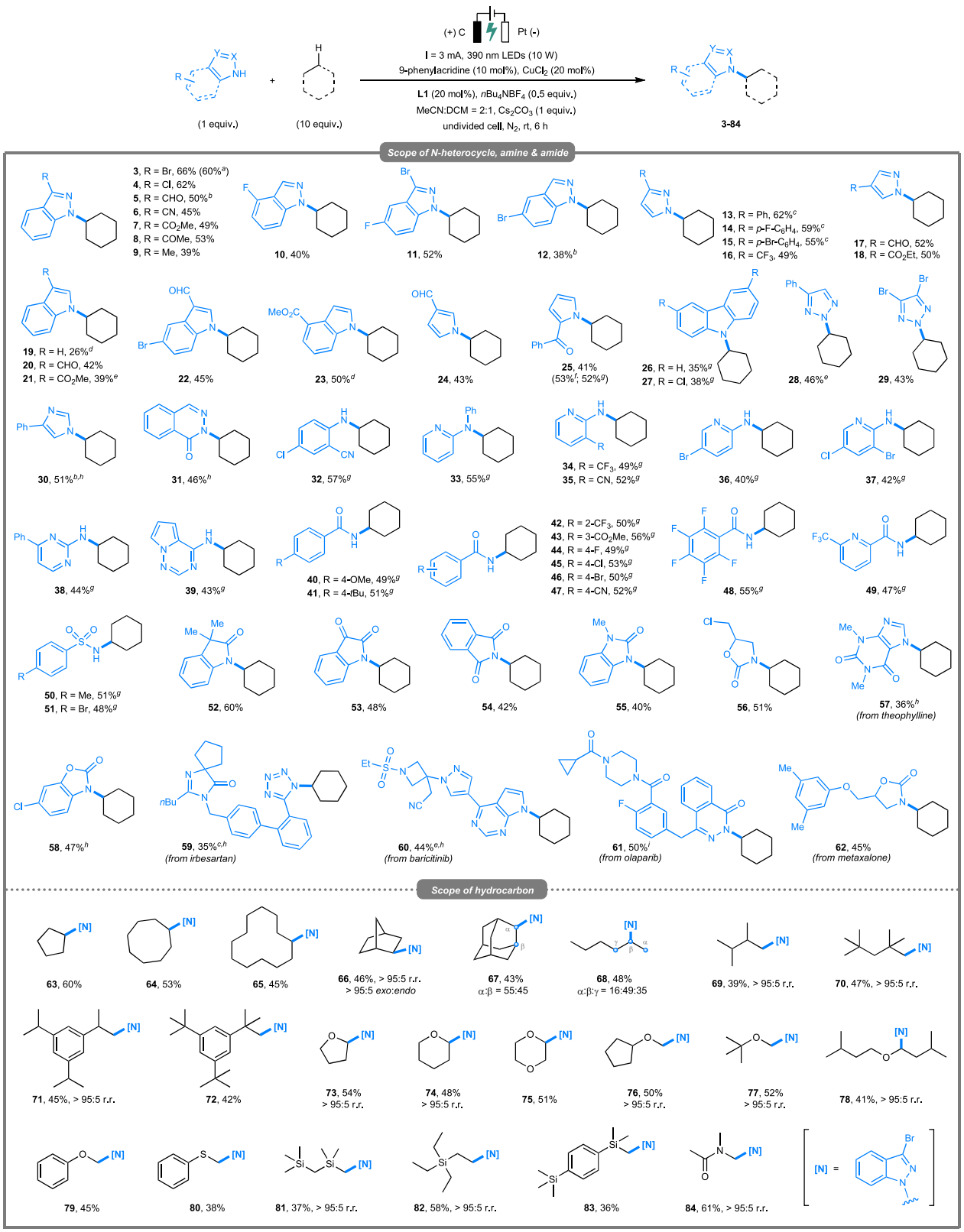

Fig. 2 | Substrate scope of C(sp^3)–H amination. Reaction conditions: undivided cell, graphite rod anode (φ = 6 mm), platinum plate cathode (15 × 10 × 0.2 mm^3), *N*-heterocycle (0.3 mmol, 1.0 equiv.), hydrocarbon (3.0 mmol, 10.0 equiv.), 9-phenylacridine (0.03 mmol, 10 mol%), $CuCl_2$ (0.06 mmol, 20 mol%), 3,4,7,8-tetramethyl-1,10-phenanthroline L1 (0.06 mmol, 20 mol%), Cs_2CO_3 (0.3 mmol, 1.0 equiv.), nBu$_4$NBF$_4$ (0.15 mmol, 0.5 equiv., 0.05 M) and anhydrous MeCN:DCM = 2:1 (*v*/*v*, 3.0 mL), constant current = 3 mA, 390 nm LEDs (10 W) under N_2 atmosphere at room temperature for 6 h (2.2 F·mol^{-1}). Yields of isolated products after chromatographic purification. Regioselectivity (r.r.) and diastereomeric ratio (d.r.) were determined by ^{1}H NMR analysis. [a]The reaction was performed on a 6.0 mmol scale. [b]nBu$_4$NClO$_4$ (0.15 mmol) as electrolyte. [c]MeCN:DCE = 2:1 (*v*/*v*, 3.0 mL) as solvent. [d]nBu$_4$NBF$_4$ (0.3 mmol) as electrolyte, BTMG (0.3 mmol) as base. [e]nBu$_4$NClO$_4$ (0.6 mmol) as electrolyte. [f]12 h. [g] nBu$_4$NBF$_4$ (0.3 mmol), Cu(OAc)$_2$ (20 mol%), dipyridine (20 mol%), NaOMe (0.3 mmol). [h]Cs_2CO_3 (0.6 mmol, 2 equiv.). [i]Cs_2CO_3 (0.9 mmol, 3 equiv.).

pyridinamide (**49**), and benzenesulfonamides (**50**–**51**) proved to be viable substrates under our reaction conditions, whereas the use of *N*-benzylbenzamide, 2-phenylacetamide, or 2-(2-(trifluoromethyl)phenyl)acetamide cannot proceed with hydrocarbon as a reaction counterpart. Furthermore, the reaction demonstrated that *N*-heterocycles such as oxindole (**52**), isatin (**53**), phthalimide (**54**), benzimidazolone (**55**) and cyclic carbamate (**56**) were tolerated as well. Moreover, we examined the late-stage modification of several bioactive pharmaceutical agents to investigate the utility of this photoelectrochemical C(sp^3)–H amination method. Theophylline, which is a commonly used alkaloid for angina treatment, was tolerated under the standard conditions to give C(sp^3)–H aminated product **57** in 36% yield. Furthermore, our photoelectrochemical method facilitated the direct installation of alkyl groups on the *N*-heterocyclic drug molecules such as irbesartan, baritinib, and olaparib, yielding the desired *N*-alkylated products (**59** to **61**) in moderate yields, thereby providing opportunities for the selective modification of structurally complicated pharmaceuticals. The oxazolidinone ring in muscle-relaxant drugs such as metaxalone underwent successful C(sp^3)–H amination with cyclohexane, producing products **62** in moderate yields. Finally, a large-scale experiment of cyclohexane (**2**) and 3-bromo-1*H*-indazole (**1**) on a 6 mmol scale was performed in order to evaluate the practical uses of this method, which could afford **3** in 60% yield (1.00 g, see the SI for more details).

Next, we explore the scope of C(sp^3)–H bond-containing hydrocarbons with 3-bromo-1*H*-indazole (**1**) under the optimal photoelectrochemical conditions (Fig. 2). In addition to cyclohexane, other cycloalkanes bearing various ring sizes, including cyclopentane (**63**), cyclooctane (**64**) and cyclododecane (**65**), are all found to be viable C(sp^3)–H substrates, which were smoothly converted into the corresponding C(sp^3)–H aminated products in 45-60% yields. Notably, norbornane readily reacted with 3-bromo-1*H*-indazole **1a** to yield the product **66** in 46% yields with high regioselectivity and stereoselectivity (>95:5 r.r, >95:5 *exo*:*endo*). Adamantane bearing a rigid cage structure also exhibited interesting regioselective characteristics, with the secondary C(sp^3)–H bond of adamantane preferentially aminated (**67**, 55:45 regioselectivity of 2°:3 °C – H bonds). These site-selective characteristics are unlike other previously reported C(sp^3)–H functionalization reactions, in which the HAT process usually occurred at the 3 °C(sp^3)–H bond[64,71]. Several acyclic alkanes were further investigated and were found to be well compatible under the standard reaction conditions, furnishing the desired amine products **68**–**70** in moderate yields. C(sp^3)–H amination of *n*-hexane gave a mixture in a combined yield of 48% (**68**). The reaction favored the methylene groups over the distal methyl group, the site selectivity of which matched our previously reported C(sp^3)–H thiolation reaction via a photo-induced Fe-LMCT process[72]. Interestingly, the reaction of 2,3-dimethylbutane (**69**) exclusively occurred at the distal methyl position rather than weaker and sterically hindered 3 °C(sp^3)–H bonds, which indicates that steric hindrance also plays a key role in affecting the regioselectivity of C–H amination. Upon using 1,3,5-triisopropylbenzene as a substrate, the C(sp^3)–H amination exclusively took place at the terminal isopropyl group (**71**), while the sterically hindered benzylic 3 °C–H bond was not observed. The C–H amination of 1,3,5-tri-*tert*-butylbenzene (**72**) with complete regioselectivity for the methyl groups. Furthermore, our method allowed the C(sp^3)–H amination to occur preferentially at the α-methylene of cyclic ethers, with the generation of the desired products **73**–**75** in moderate yields. Similar to these examples, the C(sp^3)–H amination reaction of acyclic ethers exclusively occurred at the weak and unhindered α-oxy C(sp^3)–H position, delivering the desired aminated products **76**–**79** in acceptable yields and complete site selectivity. Notably, a recent report by Noël and co-workers describes an accelerated photoelectrocatalytic C(sp^3)–H amination reaction enabled by continuous-flow synthesis, using compounds containing weak and secondary C(sp^3)–H bonds (e.g., α-oxy, α-amino, and benzylic positions) as viable substrates[19]. Our method, however, demonstrates the capability to react not only with hydrocarbons containing stronger C(sp^3)–H bonds but also with ether compounds containing both primary and secondary α-oxy C(sp^3)–H bonds.

In addition, phenyl sulfide also proved to be an effective substrate, giving the *N*-alkylated product (**80**) in 38% yield at the position adjacent to a sulfur atom. Photoelectrochemical C(sp^3)–H amination of various silanes was also investigated, with the observation of C(sp^3)–H amination products at the distal methyl groups (**81**–**82**). Notably, the reaction of tetraethylsilane (**83**) revealed that the steric effect still dominated the site selectivity, preferentially giving the distal methyl aminated product. Finally, amide compounds proved to be viable substrates. The C(sp^3)–H amination reaction of dimethylacetamide with 3-bromo-1*H*-indazole (**1**) successfully gave **84** in 61% yield with complete site selectivity for the weak and active α-amino position rather than the C–H site adjacent to the carbonyl group. Compared to the substrate scope of peroxide-based C(sp^3)–H amination reactions[32,34], our method demonstrates a substantially broader substrate range, allowing for the successful amination of hydrocarbons with aniline and aminopyridine compounds. Our method is not only applicable to the amination of simple alkanes, but can also be applied to various small organic molecules containing carbon-hydrogen bonds, including alkylated arenes, ethers, thioethers, silanes, and amides.

After exploring the substrate scope of C(sp^3)–H amination reaction, we next hypothesize that the photoelectrocatalytic strategy would provide a universal platform for the C(sp^3)–H oxygenation reaction of unactivated hydrocarbons with alcohols, thus converting these readily available substrates into valuable ether products. After a series of condition optimizations (see the SI for more details), the use of 9-phenylacridine and $(CuOTf)_2$ benzene complex as co-catalyst, 4,7-diphenyl-1,1-phenanthroline (**L2**) as supporting ligand, K_2CO_3 as base, nBu$_4$NPF$_6$ as electrolyte in a mixed solvent of MeCN/DCE (1:1, *v*/*v*) upon photoirradiation and electrolysis could significantly promote the C(sp^3)–H oxygenation reaction and obtain the target aryl ether products. Under this optimal condition, we further extend the methodology to alcohol substrates to explore the substrate scope, as shown in Fig. 3. Expectedly, a myriad of phenols containing electron-donating/neutral (**85**–**90**, **102**–**103**) and electron-withdrawing (**91**–**101**) substituents were both successfully coupled with cyclohexane to give the corresponding aryl ether products in moderate to good yields. Notably, aryl halides (**91**–**93**) groups were tolerated well in this C – O cross-coupling reaction. Other important functional groups such as trifluoromethyl (**94**), sulfonyl (**95**), cyano (**96**), alkynyl (**97**), ketone (**98**–**99**), and ester (**100**) were all compatible under the photoelectrochemical conditions. A key intermediate in the production and modification of lipid-lowering drug fenofibrate can also react (**98**). Notably, both aryl boronate ester (**101**) and amide (**102**–**103**) moieties were also tolerated. This method can be well applied to polycyclic aromatic ring (**104**). It was notable to see that hydroxy-substituted heterocycles containing benzooxazole (**105**), isobenzofuranone (**106**), dihydrobenzofuran (**107**), and dihydroquinolinone (**108**, a crucial intermediate in the synthesis of the antipsychotic medication aripiprazole) moieties were also compatible to afford the corresponding aromatic ether products (**105**–**108**) in moderate yields. Furthermore, the current C(sp^3)–O cross-coupling method was applied to the late-stage etherification of natural products and molecular drugs. Natural phenolic compounds such as raspberry ketone (**109**) and estrone (**110**), as well as pharmaceutically relevant substances such as *L*-tyrosine derivatives (**111**) and ezetimide (**112**), underwent the photoelectrochemical reactions with cyclohexane to gain the corresponding aryl ether products in moderate yields. Alkanols and carboxylic acids were also tested under the standard conditions for C – O bond construction, but the reactions did not provide any positive results. In addition to C – O bond formation, the scope of other nucleophiles for the

https://doi.org/10.1038/s41467-025-60429-6

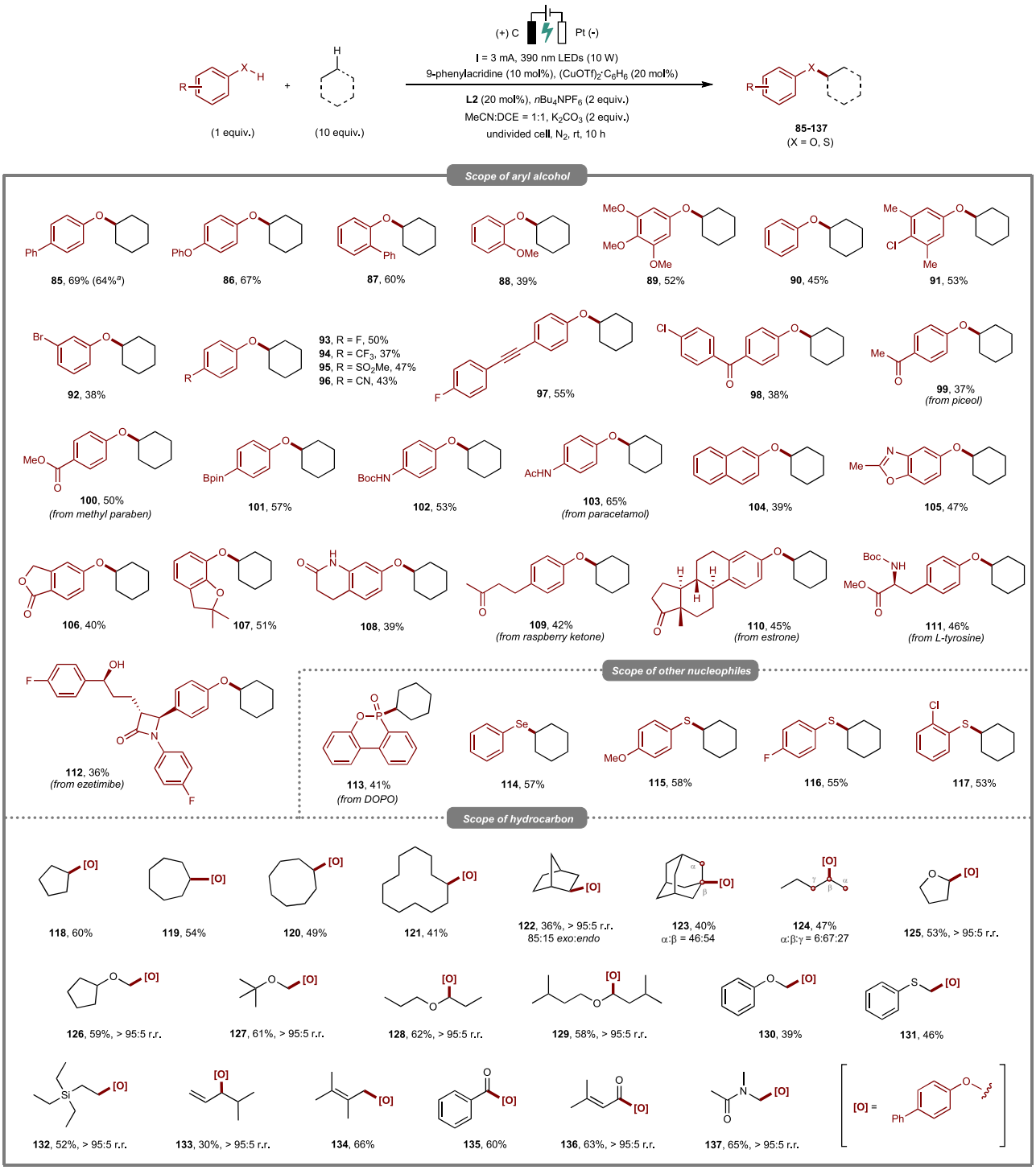

Fig. 3 | Substrate scope of C(sp^3)–H oxygenation. Reaction conditions: undivided cell, graphite rod anode (φ = 6 mm), platinum plate cathode (15 × 10 × 0.2 mm^3), aryl alcohol (0.3 mmol, 1.0 equiv.), hydrocarbon (3.0 mmol, 10.0 equiv.), 9-phenylacridine (0.03 mmol, 10 mol%), $(CuOTf)_2{\cdot}C_6H_6$ (0.06 mmol, 20 mol%), 4,7-diphenyl-1,1-phenanthroline **L2** (0.06 mmol, 20 mol%), K_2CO_3 (0.3 mmol, 1.0 equiv.), nBu_4NPF_6 (0.60 mmol, 2.0 equiv., 0.2 M) and anhydrous MeCN:DCE = 1:1 (v/v, 3.0 mL), constant current = 3 mA, 390 nm LEDs (10 W) under N_2 atmosphere at room temperature for 10 h (3.7 F·mol^{-1}). Yields of isolated products after chromatographic purification. Regioselectivity (r.r.) and diastereomeric ratio (d.r.) were determined by ^{1}H NMR analysis. [a]The reaction was performed on a 6.0 mmol scale.

construction of C(sp^3)–P, C(sp^3)–Se and C(sp^3)–S bonds was subsequently explored. The flame retardant intermediates 9,10-dihydro-9-oxa-10-phosphaphenanthrene 10-oxide (DOPO) and phenylselenol could be reacted well and provided **113** and **114** in moderate yields. Thiophenols containing either electron-donating (**115**) or electron-withdrawing (**116**–**117**) substituents were both coupled to give the corresponding thioethers in acceptable yields. The success of all the above-mentioned substrates, many of which contain sensitive alkyne, carbonyl, halide or heterocyclic groups, underscores the high chemoselectivity and functional group compatibility of our developed method.

Next, the scope of C − H bond-containing hydrocarbons for C(sp^3)–O bond formation was assessed. As shown in Fig. 3, various cycloalkanes were all found to be suitable C(sp^3)–H substrates

(**118**–**121**), which were smoothly converted into the corresponding alkyl aryl ethers in 41-60% yields. Norbornane, as a viable substrate, could readily react with 4-phenylphenol to give the corresponding product **122** in 36% yield. Our method also showed the successful validation of C(sp^3)–H oxygenation of adamantane (**123**), with the occurrence of HAT process at the tertiary C – H bond. Moreover, the C(sp^3)–O coupling of *n*-pentane (**124**) was found to effectively afford a mixture of ether products in a combined yield of 48%, and the reaction favored the methylene groups over the distal methyl group. Similar to C(sp^3)–H amination protocol, our method allowed the C(sp^3)–H oxygenation reaction to occur preferentially at the α-oxy position of cyclic and acyclic ethers (**125**–**130**), indicating that the reaction favors the C(sp^3)–H functionalization of weak and sterically unhindered C(sp^3)–H bonds. Thioanisole proceeded well under the standard conditions (**131**). Notably, the C(sp^3)–O coupling of tetraethylsilane (**132**) revealed that the steric effect still dominated the site selectivity, preferentially giving the distal methyl C(sp^3)–O coupling product. The reaction of 4-methyl-1-pentene was also feasible (**133**), with the occurrence of C(sp^3)–H oxygenation exclusively at the weak allylic position. 2,3-Dimethyl-2-butene was demonstrated to be compatible with the method, furnishing the desired C(sp^3)–O coupling product **134** in 66% yield. It is noteworthy that the C(sp^3)–O coupling of aldehyde substrate (**135**–**136**) delivered the corresponding ester products in moderate yields with complete site-selectivity at the C(acyl)–H bond. Furthermore, the reaction of dimethylacetamide with 4-phenylphenol at the α-amino position was also exclusively observed (**137**).

Mechanistic studies

In order to get a deeper insight into the reaction mechanism, several mechanistic experiments were then carried out, as shown in Fig. 4. Firstly, the model reactions of C(sp^3)–H amination and etherification were both strongly suppressed by a radical trapping experiment using 2,2,6,6-tetramethylpiperidine-1-oxyl (TEMPO) as the radical scavenger (Fig. 4a). The formation of the corresponding adduct 1-(cyclohexyloxy)-2,2,6,6-tetramethylpiperidine **139** between TEMPO and cyclohexyl radical was observed and isolated (see the SI for more details), with no detection of the expected C(sp^3)–H amination and etherification products (**3** and **85**). Both of these results indicated that a radical pathway and key alkyl radical species might be involved in these two photoelectrochemical transformations. In order to further capture the key radical intermediates, an electron paramagnetic resonance (EPR) experiment was performed with the addition of a free radical spin trap 5,5-dimethyl-1-pyrroline *N*-oxide (DMPO), as shown in Fig. 4b. The EPR spectroscopy studies revealed that a carbon-centered radical species were generated from the corresponding alkane substrate via an intermolecular HAT process and rapidly captured by DMPO to form relatively stable free radicals ($g = 2.0074$, $A_N = 14.62$ G, $A_H = 21.54$ G)[73–76].

To gain more insights into the hydrogen atom transfer (HAT) species, several control experiments were conducted in the absence of *N*-heterocycles or alcohols, as shown in Fig. 4c. Considering nitrogen radicals are prone to undergoing the HAT process[65,66], the photoelectrochemical reaction of 9-phenylacridine with cyclohexane (**2**) was then conducted in the absence of copper catalyst and supporting ligand, and yielded compound **141** in 16% yield as the major product. Notably, the yield of **141** was increased to 53% without constant current. This result indicated that the HAT species in this reaction is highly likely to be the nitrogen radical species formed by photoexcitation of 9-phenylacridine (for the UV-Vis spectrum, see the SI for more details). The nitrogen radical extracted hydrogen from the alkane substrate to generate a transient alkyl radical (**143**) and a persistent triarylmethyl (trityl) radical (**142**), which would further undergo radical-radical coupling to release the final product **141**. Similar results were afforded with the utilization of mesitylene (**144**) or 1,3,5-trimethoxybenzene (**146**) as the hydrocarbon substrate instead of cyclohexane, and the reactions successfully delivered the corresponding radical addition products **145** and **147** in 50% and 45% yields, respectively. Support for this mechanism was also provided by the formation of isotopically labeled product **141-[D]** in 56% yield upon photo-induced reaction of 9-phenylacridine with deuterated cyclohexane (**2-d_{12}**). The lower N–H deuterium incorporation (~12% D) obtained in the product **141-[D]** may be due to fast deuterium-proton exchange. Kinetic isotope effect (KIE) experiments were subsequently performed to explore whether the HAT step was the rate-determining step of the overall reaction process, as shown in Fig. 4d. The photoelectrochemical reaction of 3-bromo-1*H*-indazole (**1**) with equal amounts of cyclohexane (**2**) and deuterated cyclohexane (**2-d_{12}**) for 3 h under the standard conditions produced a mixture of C–H amination products **3** and isotopically labeled **3-d_{11}** in 32% yield. The obtained ratio ($k_H/k_D = 2.1$) suggests that the HAT process is a turnover-limiting step in the overall reaction. A similar ratio ($k_H/k_D = 1.8$) was obtained for the KIE of C(sp^3)–H etherification under optimal reaction conditions, suggesting that the hydrogen/deuterium atom extraction step may also be turnover-limiting.

Having demonstrated the key intermediates in the reaction process, we next set out to investigate the origin of the site selectivity produced in the C(sp^3)–H functionalization reaction. As shown in Fig. 4e, we utilized 2,3-dimethylbutane (DMB, **148**) as a standard substrate to probe the site selectivity[74,77,78]. The control reaction showed that the addition of phenyl acrylate (**149**) to the standard photoelectrochemical system containing DMB and 3-bromo-1*H*-indazole (**1**) successfully afforded C(sp^3)–H alkylation product **150** in 37% yield, with the alkylation preferentially occurring at 3 °C–H bond (intrinsic selectivity of 1°/3° is 1:13, which was calculated by the number of available C(sp^3)–H bonds). Electrolysis and photoirradiation of the same starting materials in the presence of 9-phenylacridine (without copper) also afforded the C(sp^3)–H alkylated product **150** in 42% yield. The above results confirm the reversible HAT process for the formation of carbon-centered radicals and imply that the use of radical acceptors largely influences the site selectivity[43,72].

To further prove the effectiveness of 9-phenylacridine as a d-HAT reagent, a series of radical-mediated C(sp^3)–H functionalization reactions of hydrocarbons were conducted under photo-induced reaction conditions (Fig. 4f). The use of alkynyl sulfone (**151**) as an efficient radical acceptor could successfully deliver the corresponding C(sp^3)–H alkynylation product **152** in 70% yield. Although the use of diphenyl disulfide (**153**) showed less efficiency for C(sp^3)–H thiolation, the desired C(sp^3)–H selenylation reaction could proceed very well to give the alkyl selenide product **114** in 73% yield. Furthermore, a divided-cell experiment was carried out (Fig. 4g), with the placement of substrates **1** and **2** along with 9-phenylacridine, $CuCl_2$, **L1**, Cs_2CO_3, nBu$_4$NBF$_4$ and solvent in the anode chamber, while nBu$_4$NBF$_4$ and solvent were added into the cathode chamber. As expected, the desired C(sp^3)–H amination product **3** was detected in the anode chamber with 40% yield, which suggested that the photoelectrochemical C(sp^3)–H amination occurred mainly around the graphite rod anode. Similarly, the formation of the desired product **85** was observed in the anode chamber under the standard conditions of C(sp^3)–H etherification, revealing that the photoelectrochemical C(sp^3)–H etherification also took place mainly around the graphite rod anode rather than around the platinum plate cathode.

Based on the above mechanistic studies and relevant literature reports[59,79], we proposed a plausible reaction mechanism for the photoelectrochemical C(sp^3)–H amination and etherification. Taking the C(sp^3)–H amination reaction as an example, which is outlined in Fig. 5, we postulated that the reaction is initiated from the excitation of the acridine-based photocatalyst (**A**) to generate the excited species **B**. Then, the excited species **B** undergoes a hydrogen atom transfer (HAT) process with unactivated hydrocarbons to release a key carbon-centered radical intermediate (**D**), while generating a persistent triarylmethyl (trityl) radical (**142**)[80–82]. Subsequently, intermediate **142** is

https://doi.org/10.1038/s41467-025-60429-6

electrochemically oxidized to triarylmethyl cation at the anode surface, followed by an elimination process to regenerate the 9-phenylacridine photocatalyst. On the other hand, the released carbon-centered radical **D** reacts with the copper complex **H** to generate a Cu^{III} species (**I**), which undergoes reductive elimination to produce the C(sp^3)–H amination product (**J**). Furthermore, the

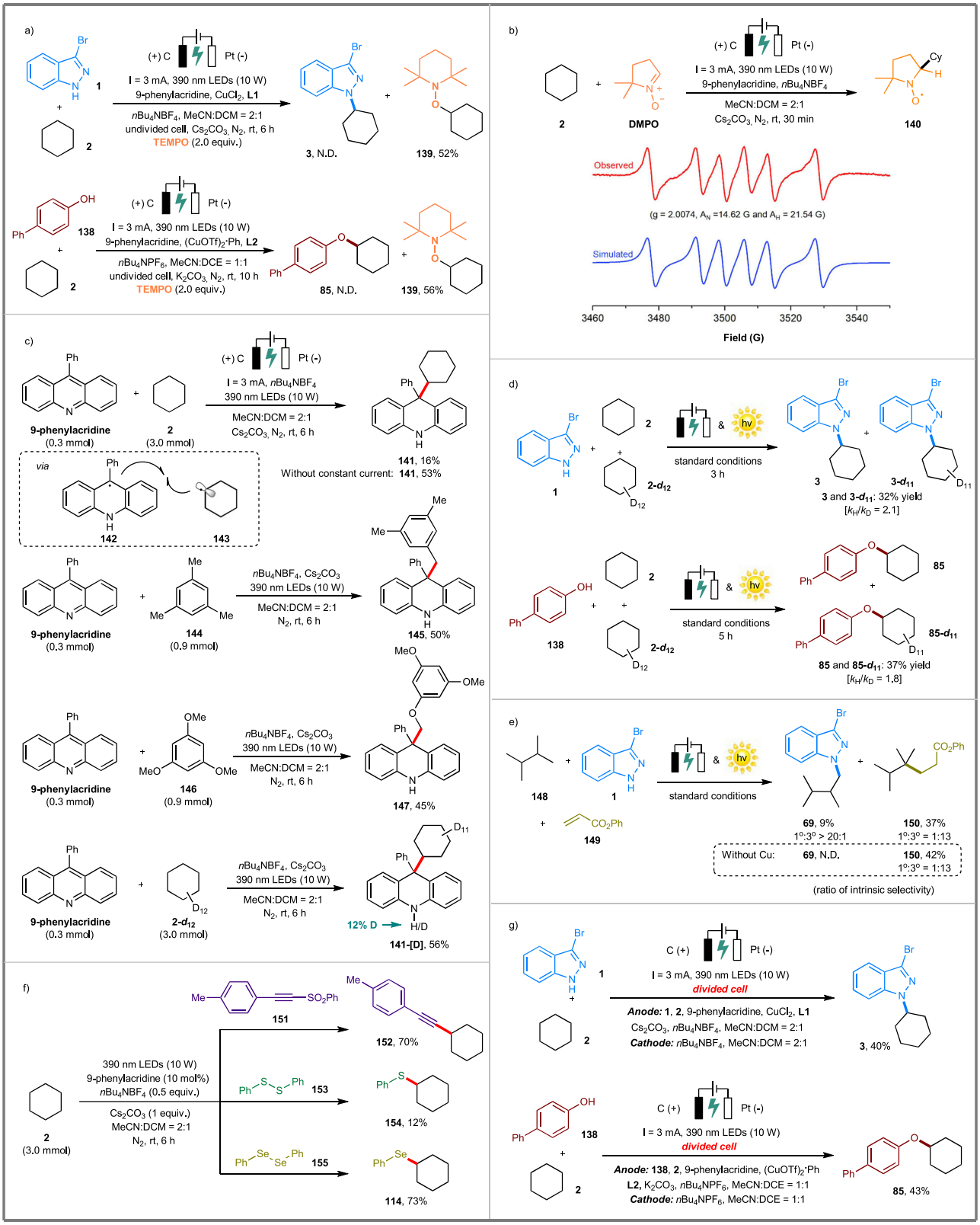

Fig. 4 | Mechanistic studies. a Capture of alkyl radical by TEMPO, **b** Electron paramagnetic resonance (EPR) experiment, **c** Capture of trityl radical, **d** Kinetic isotopic effect (KIE) experiment, **e** Investigation of the site selectivity, **f** Photo-induced C(sp^3)–H alkynylation, thiolation and selenylation reactions enabled by 9-phenylacridine as d-HAT photocatalyst, **g** Divided-cell experiment.

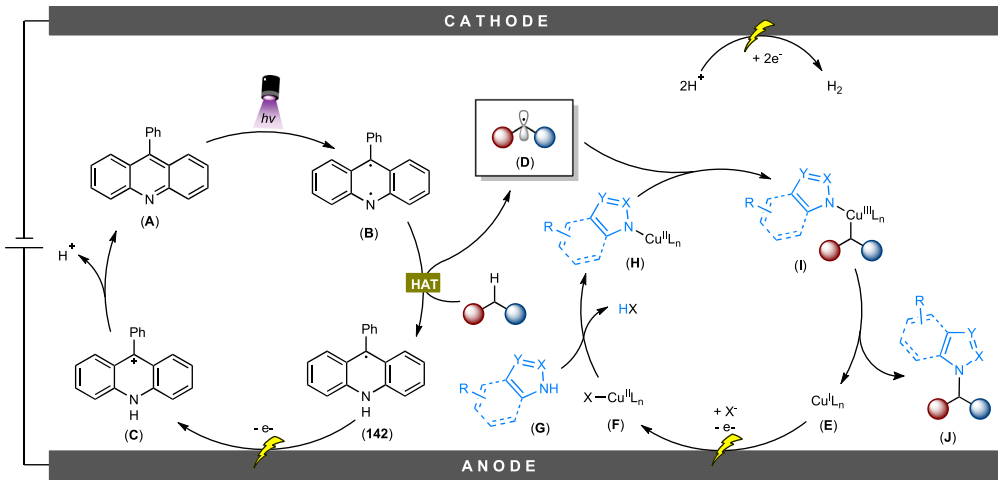

Fig. 5 | Plausible reaction mechanism. The proposed mechanism includes a photoelectrocatalytic cycle of 9-phenylacridine and a copper-catalyzed cycle, with the main electrochemical processes occurring at the anode surface.

reduced catalyst **E** is electrochemically oxidized to a Cu^{II} species **F** on the anode, and intermediate **F** reacts with *N*-heterocycles to form species **H** and closes both catalytic cycles.

Discussion

In summary, we have developed a mild and efficient C(sp^3)–H functionalization method enabled by a photoelectrochemical strategy. Using 9-phenylacridine as a direct hydrogen atom transfer (d-HAT) reagent under 390 nm LED light irradiation and electrolysis, this synthetic approach is capable of preparing various types of aliphatic *N*-heterocycle and ether compounds from hydrocarbons. Our methodology greatly extends the range of available substrates not only for *N*-heterocycles and phenol derivatives, but also for a wide variety of C(sp^3)–H compounds, including unactivated alkanes, ethers, thioethers, silanes, and amides. The mild reaction conditions, operational simplicity, remarkably broad substrate scope (>135 examples), as well as scalability, demonstrate that the method has potential for industrial application. Importantly, the reaction exhibits unconventional site selectivity, with the occurrence of both C(sp^3)–H amination and etherification preferentially at the sterically unhindered position. Considering the importance and versatility of *N*-heterocycle, amine, amide, and ether compounds as important functional molecules in organic synthesis, we believe that the method we have developed has the potential to be a versatile tool for chemists, offering a plethora of opportunities for selective installation of valuable functional groups at the late stage. Further development of other types of photo-induced and electrochemical reactions is still underway in our lab.

Methods

General procedure for photoelectrochemical C(sp^3)–H amination

In a glove box filled with nitrogen, a 20 mL oven-dried quartz tube with a stir bar was charged the *N*-heterocycle substrate (0.3 mmol, 1 equiv.), unactivated alkane (3.0 mmol, 10 equiv.), 9-phenylacridine (0.03 mmol, 10 mol%), $CuCl_2$ (0.06 mmol, 20 mol%), 3,4,7,8-tetramethyl-1,10-phenanthroline **L1** (0.06 mmol, 20 mol%), Cs_2CO_3 (0.3 mmol, 1 equiv.), nBu$_4$NBF$_4$ (0.15 mmol, 0.5 equiv., 0.05 M) and anhydrous MeCN:DCM = 2:1 (v/v, 3.0 mL). The tube was equipped with a carbon rod (φ = 6 mm) anode and a platinum plate cathode(15 × 10 × 0.2 mm^3), and the tubes were then sealed and taken out from the glove box. The reaction mixture was irradiated with 390 nm LED lamps (10 W) and 3.0 mA electrolysis for 6 h. The distance between electrodes was approximately 0.5 cm, and the length below the liquid surface was 1.0 cm. Upon completion of the reaction, the reaction yield was monitored by TLC or GC-MS. Subsequently, the solvent was removed under reduced pressure, and the resulting mixture was purified by column chromatography on silica gel (eluted with petroleum ether/ethyl acetate) to afford the desired pure product.

General procedure for photoelectrochemical C(sp^3)–H etherification

In a glove box filled with nitrogen, a 20 mL oven-dried quartz tube with a stir bar was charged the phenol or phenylthiophenol substrate (0.3 mmol, 1 equiv), unactivated alkane (3.0 mmol, 10 equiv), 9-phenylacridine (0.03 mmol, 10 mol%), $(CuOTf)_2{\cdot}C_6H_6$ (0.06 mmol, 20 mol%), 4,7-diphenyl-1,1-phenanthroline **L2** (0.06 mmol, 20 mol%), K_2CO_3 (0.6 mmol, 2 equiv.), nBu$_4$NPF$_6$ (0.6 mmol, 2 equiv., 0.2 M) and anhydrous MeCN:DCE = 1:1 (v/v, 3.0 mL). The tube was equipped with a carbon rod (φ = 6 mm) anode and a platinum plate (15 × 10 × 0.2 mm^3) cathode, and the tubes were then sealed and taken out the glove box. The reaction mixture was irradiated with 390 nm LED lamps (10 W) and 3.0 mA electrolysis for 10 h. The distance between electrodes was approximately 0.5 cm, and the length below the liquid surface was 1.0 cm. Upon completion of the reaction, the reaction yield was monitored by TLC or GC-MS. Subsequently, the solvent was removed under reduced pressure, and the resulting mixture was purified by column chromatography on silica gel (eluted with petroleum ether/ethyl acetate) to afford the desired pure product.

Data availability

Materials and methods, optimization studies, experimental procedures, mechanistic studies, ^{1}H NMR spectra, ^{13}C NMR spectra and mass spectrometry data generated in this study are provided in the Supplementary Information file. Source data are provided with this paper. Data supporting the findings of this manuscript are also available from the corresponding author upon request. Source data are provided with this paper.

References

1. Hartwig, J. F. & Larsen, M. A. Undirected, Homogeneous C–H bond functionalization: challenges and opportunities. *ACS Cent. Sci.* **2**, 281–292 (2016).
2. Davies, H. M. L. & Manning, J. R. Catalytic C–H functionalization by metal carbenoid and nitrenoid insertion. *Nature* **451**, 417–424 (2008).
3. Doyle, M. P., Duffy, R., Ratnikov, M. & Zhou, L. Catalytic carbene insertion into C–H bonds. *Chem. Rev.* **110**, 704–724 (2010).

4. He, J., Wasa, M., Chan, K. S. L., Shao, Q. & Yu, J.-Q. Palladium-catalyzed transformations of alkyl C–H bonds. *Chem. Rev.* **117**, 8754–8786 (2017).
5. Gutekunst, W. R. & Baran, P. S. C–H functionalization logic in total synthesis. *Chem. Soc. Rev.* **40**, 1976–1991 (2011).
6. Godula, K. & Sames, D. C-H bond functionalization in complex organic synthesis. *Science* **312**, 67–72 (2006).
7. Guillemard, L., Kaplaneris, N., Ackermann, L. & Johansson, M. J. Late-stage C–H functionalization offers new opportunities in drug discovery. *Nat. Rev. Chem.* **5**, 522–545 (2021).
8. Kuninobu, Y. & Sueki, S. C–H bond transformations leading to the synthesis of organic functional materials. *Synthesis* **47**, 3823–3845 (2015).
9. Kawamata, Y. et al. Scalable, electrochemical oxidation of unactivated C–H bonds. *J. Am. Chem. Soc.* **139**, 7448–7451 (2017).
10. Roth, H. G., Romero, N. A. & Nicewicz, D. A. Experimental and calculated electrochemical potentials of common organic molecules for applications to single-electron redox chemistry. *Synlett* **27**, 714–723 (2016).
11. Cao, H., Tang, X., Tang, H., Yuan, Y. & Wu, J. Photoinduced intermolecular hydrogen atom transfer reactions in organic synthesis. *Chem. Catal.* **1**, 523–598 (2021).
12. Capaldo, L., Ravelli, D. & Fagnoni, M. Direct photocatalyzed hydrogen atom transfer (HAT) for aliphatic C–H bonds elaboration. *Chem. Rev.* **122**, 1875–1924 (2022).
13. Golden, D. L., Suh, S.-E. & Stahl, S. S. Radical C(sp^3)–H functionalization and cross-coupling reactions. *Nat. Rev. Chem.* **6**, 405–427 (2022).
14. Zhang, Z., Chen, P. & Liu, G. Copper-catalyzed radical relay in C(sp^3)–H functionalization. *Chem. Soc. Rev.* **51**, 1640–1658 (2022).
15. Wang, F., Chen, P. & Liu, G. Copper-catalyzed radical relay for asymmetric radical transformations. *Acc. Chem. Res.* **51**, 2036–2046 (2018).
16. Yi, H. et al. Recent advances in radical C–H activation/radical cross-coupling. *Chem. Rev.* **117**, 9016–9085 (2017).
17. Zhang, C., Li, Z.-L., Gu, Q.-S. & Liu, X.-Y. Catalytic enantioselective C(sp^3)–H functionalization involving radical intermediates. *Nat. Commun.* **12**, 475 (2021).
18. Cernak, T., Dykstra, K. D., Tyagarajan, S., Vachal, P. & Krska, S. W. The medicinal chemist's toolbox for late stage functionalization of drug-like molecules. *Chem. Soc. Rev.* **45**, 546–576 (2016).
19. Ioannou, D. I., Capaldo, L., Sanramat, J., Reek, J. N. H. & Noël, T. Accelerated electrophotocatalytic C(sp^3)–H heteroarylation enabled by an efficient continuous-flow reactor. *Angew. Chem. Int. Ed.* **62**, e202315881 (2023).
20. Suh, S.-E., Nkulu, L. E., Lin, S., Krska, S. W. & Stahl, S. S. Benzylic C–H isocyanation/amine coupling sequence enabling high-throughput synthesis of pharmaceutically relevant ureas. *Chem. Sci.* **12**, 10380–10387 (2021).
21. Chen, X., Lian, Z. & Kramer, S. Enantioselective intermolecular radical amidation and amination of benzylic C–H bonds via dual copper and photocatalysis. *Angew. Chem. Int. Ed.* **62**, e202217638 (2023).
22. Chen, S.-J., Golden, D. L., Krska, S. W. & Stahl, S. S. Copper-catalyzed cross-coupling of benzylic C–H bonds and azoles with controlled N-site selectivity. *J. Am. Chem. Soc.* **143**, 14438–14444 (2021).
23. Bao, X., Wang, Q. & Zhu, J. Copper-catalyzed remote C(sp^3)–H azidation and oxidative trifluoromethylation of benzohydrazides. *Nat. Commun.* **10**, 769 (2019).
24. Suh, S.-E. et al. Site-selective copper-catalyzed azidation of benzylic C–H bonds. *J. Am. Chem. Soc.* **142**, 11388–11393 (2020).
25. Chen, Y., Yang, B., Li, Q.-Y., Lin, Y.-M. & Gong, L. Selectfluor®-enabled photochemical selective C(sp^3)–H(sulfonyl)amidation. *Chem. Commun.* **59**, 118–121 (2023).
26. Hou, Z.-W. et al. Site-selective electrochemical benzylic C–H amination. *Angew. Chem. Int. Ed.* **60**, 2943–2947 (2021).
27. Das, M., Zamani, L., Bratcher, C. & Musacchio, P. Z. Azolation of benzylic C–H bonds via photoredox-catalyzed carbocation generation. *J. Am. Chem. Soc.* **145**, 3861–3868 (2023).
28. Ruos, M. E., Kinney, R. G., Ring, O. T. & Doyle, A. G. A general photocatalytic strategy for nucleophilic amination of primary and secondary benzylic C–H bonds. *J. Am. Chem. Soc.* **145**, 18487–18496 (2023).
29. Clark, J. R., Feng, K., Sookezian, A. & White, M. C. Manganese-catalysed benzylic C(sp^3)–H amination for late-stage functionalization. *Nat. Chem.* **10**, 583–591 (2018).
30. Park, Y., Kim, Y. & Chang, S. Transition metal-catalyzed C–H amination: scope, mechanism, and applications. *Chem. Rev.* **117**, 9247–9301 (2017).
31. Tran, B. L., Li, B., Driess, M. & Hartwig, J. F. Copper-catalyzed intermolecular amidation and imidation of unactivated alkanes. *J. Am. Chem. Soc.* **136**, 2555–2563 (2014).
32. Wang, C.-S., Wu, X.-F., Dixneuf, P. H. & Soulé, J.-F. Copper-catalyzed oxidative dehydrogenative C(sp^3)–H bond amination of (cyclo) alkanes using NH-heterocycles as amine sources. *ChemSusChem* **10**, 3075–3082 (2017).
33. Bakhoda, A. G. et al. Copper-catalyzed C(sp^3)–H amidation: sterically driven primary and secondary C–H site-selectivity. *Angew. Chem. Int. Ed.* **58**, 3421–3425 (2019).
34. Zheng, Y.-M., Narobe, R., Donabauer, K., Yakubov, S. & König, B. Copper(II)-photocatalyzed N–H alkylation with alkanes. *ACS Catal.* **10**, 8582–8589 (2020).
35. Ide, T. et al. Late-stage intermolecular allylic C–H amination. *J. Am. Chem. Soc.* **143**, 14969–14975 (2021).
36. Lee, J., Jin, S., Kim, D., Hong, S. H. & Chang, S. Cobalt-catalyzed intermolecular C–H amidation of unactivated alkanes. *J. Am. Chem. Soc.* **143**, 5191–5200 (2021).
37. Wang, Q., Ni, S., Yu, L., Pan, Y. & Wang, Y. Photoexcited direct amination/amidation of inert Csp^3–H bonds via tungsten–nickel catalytic relay. *ACS Catal.* **12**, 11071–11077 (2022).
38. Wang, Q., Ni, S., Wang, X., Wang, Y. & Pan, Y. Visible-light-mediated tungsten-catalyzed C-H amination of unactivated alkanes with nitroarenes. *Sci. China Chem.* **65**, 678–685 (2022).
39. Boquet, V. et al. Rhodium(II)-catalyzed selective C(sp^3)–H amination of alkanes. *Eur. J. Org. Chem.* **26**, e202300352 (2023).
40. Liu, Y. et al. Iron-catalyzed primary amination of C(sp^3)–H bonds. *J. Am. Chem. Soc.* **146**, 24863–24870 (2024).
41. Salvador, T. K. et al. Copper catalyzed sp^3 C–H etherification with acyl protected phenols. *J. Am. Chem. Soc.* **138**, 16580–16583 (2016).
42. Hu, H. et al. Copper-catalysed benzylic C–H coupling with alcohols via radical relay enabled by redox buffering. *Nat. Catal.* **3**, 358–367 (2020).
43. Zhong, P.-F. et al. Photoelectrochemical oxidative C(sp^3)–H borylation of unactivated hydrocarbons. *Nat. Commun.* **14**, 6530 (2023).
44. Malapit, C. A. et al. Advances on the merger of electrochemistry and transition metal catalysis for organic synthesis. *Chem. Rev.* **122**, 3180–3218 (2022).
45. Yan, M., Kawamata, Y. & Baran, P. S. Synthetic organic electrochemical methods since 2000: on the verge of a renaissance. *Chem. Rev.* **117**, 13230–13319 (2017).
46. Pollok, D. & Waldvogel, S. R. Electro-organic synthesis—a 21st century technique. *Chem. Sci.* **11**, 12386–12400 (2020).
47. Zhu, C., Ang, N. W. J., Meyer, T. H., Qiu, Y. & Ackermann, L. Organic electrochemistry: molecular syntheses with potential. *ACS Cent. Sci.* **7**, 415–431 (2021).
48. Cheng, X. et al. Recent applications of homogeneous catalysis in electrochemical organic synthesis. *CCS Chem.* **4**, 1120–1152 (2022).

49. Yuan, Y., Yang, J. & Lei, A. Recent advances in electrochemical oxidative cross-coupling with hydrogen evolution involving radicals. *Chem. Soc. Rev.* **50**, 10058–10086 (2021).
50. Meyer, T. H., Choi, I., Tian, C. & Ackermann, L. Powering the future: how can electrochemistry make a difference in organic synthesis. *Chem* **6**, 2484–2496 (2020).
51. Siu, J. C., Fu, N. & Lin, S. Catalyzing electrosynthesis: a homogeneous electrocatalytic approach to reaction discovery. *Acc. Chem. Res.* **53**, 547–560 (2020).
52. Nutting, J. E., Rafiee, M. & Stahl, S. S. Tetramethylpiperidine *N*-oxyl (TEMPO), phthalimide *N*-oxyl (PINO), and related *N*-oxyl species: electrochemical properties and their use in electrocatalytic reactions. *Chem. Rev.* **118**, 4834–4885 (2018).
53. Francke, R. & Little, R. D. Redox catalysis in organic electrosynthesis: basic principles and recent developments. *Chem. Soc. Rev.* **43**, 2492–2521 (2014).
54. Liu, J., Lu, L., Wood, D. & Lin, S. New redox strategies in organic synthesis by means of electrochemistry and photochemistry. *ACS Cent. Sci.* **6**, 1317–1340 (2020).
55. Barham, J. P. & König, B. Synthetic Photoelectrochemistry. *Angew. Chem. Int. Ed.* **59**, 11732–11747 (2020).
56. Huang, H., Steiniger, K. A. & Lambert, T. H. Electrophotocatalysis: combining light and electricity to catalyze reactions. *J. Am. Chem. Soc.* **144**, 12567–12583 (2022).
57. Yu, Y., Guo, P., Zhong, J.-S., Yuan, Y. & Ye, K.-Y. Merging photochemistry with electrochemistry in organic synthesis. *Org. Chem. Front.* **7**, 131–135 (2020).
58. Singh, P., König, B. & Shaikh, A. C. Electro-photochemical functionalization of C(sp^3)–H bonds: synthesis toward sustainability. *JACS Au* **4**, 3340–3357 (2024).
59. Holmberg-Douglas, N. & Nicewicz, D. A. Photoredox-catalyzed C–H functionalization reactions. *Chem. Rev.* **122**, 1925–2016 (2022).
60. Jia, P. et al. Light-promoted bromine-radical-mediated selective alkylation and amination of unactivated C(sp^3)–H bonds. *Chem.* **6**, 1766–1776 (2020).
61. Deng, H.-P., Zhou, Q. & Wu, J. Microtubing-reactor-assisted aliphatic C–H functionalization with HCl as a hydrogen-atom-transfer catalyst precursor in conjunction with an organic photoredox catalyst. *Angew. Chem. Int. Ed.* **57**, 12661–12665 (2018).
62. Li, D.-S. et al. Stop-flow microtubing reactor-assisted visible light-induced hydrogen-evolution cross coupling of heteroarenes with C(sp^3)–H bonds. *ACS Catal.* **12**, 4473–4480 (2022).
63. Schlegel, M., Qian, S. & Nicewicz, D. A. Aliphatic C–H functionalization using pyridine *N*-oxides as H-atom abstraction agents. *ACS Catal.* **12**, 10499–10505 (2022).
64. Wang, B. et al. Photoinduced site-selective functionalization of aliphatic C–H bonds by pyridine *N*-oxide based HAT catalysts. *ACS Catal.* **12**, 10441–10448 (2022).
65. Kwon, K., Simons, R. T., Nandakumar, M. & Roizen, J. L. Strategies to generate nitrogen-centered radicals that may rely on photoredox catalysis: development in reaction methodology and applications in organic synthesis. *Chem. Rev.* **122**, 2353–2428 (2022).
66. Matsumoto, A. & Maruoka, K. Design of organic radical cations as potent hydrogen-atom transfer catalysts for C–H functionalization. *Asian J. Org. Chem.* **13**, e202300580 (2024).
67. Entgelmeier, L.-M. et al. Zwitterionic acridinium amidate: a nitrogen-centered radical catalyst for photoinduced direct hydrogen atom transfer. *Angew. Chem. Int. Ed.* **63**, e202404890 (2024).
68. Wang, Y. et al. A HAT process of *N*-pyridyl radical cations for the synthesis of benzophenone-type bioisosteres. *Org. Chem. Front.* **11**, 5712–5719 (2024).
69. Bhatt, K. et al. Photocatalytic decarboxylative alkylation of cyclic imine–BF_3 complexes: a modular route to functionalized azacycles. *J. Am. Chem. Soc.* **146**, 26331–26339 (2024).
70. Korpusik, A. B. et al. Degradation of polyacrylates by one-pot sequential dehydrodecarboxylation and ozonolysis. *J. Am. Chem. Soc.* **145**, 10480–10485 (2023).
71. Yang, H.-B., Feceu, A. & Martin, D. B. C. Catalyst-controlled C–H functionalization of adamantanes using selective H-atom transfer. *ACS Catal.* **9**, 5708–5715 (2019).
72. Tu, J.-L., Hu, A.-M., Guo, L. & Xia, W. Iron-catalyzed C(Sp^3)–H borylation, thiolation, and sulfinylation enabled by photoinduced ligand-to-metal charge transfer. *J. Am. Chem. Soc.* **145**, 7600–7611 (2023).
73. Liu, Y. et al. Time-resolved EPR revealed the formation, structure, and reactivity of *N*-centered radicals in an electrochemical C(sp^3)–H arylation reaction. *J. Am. Chem. Soc.* **143**, 20863–20872 (2021).
74. An, Q. et al. Identification of alkoxy radicals as hydrogen atom transfer agents in Ce-catalyzed C–H functionalization. *J. Am. Chem. Soc.* **145**, 359–376 (2023).
75. Bao, Y. et al. Copper-catalyzed radical methylation/C–H amination/oxidation cascade for the synthesis of quinazolinones. *J. Org. Chem.* **80**, 4736–4742 (2015).
76. Oyama, R. & Abe, M. Reactivity and product analysis of a pair of cumyloxyl and *tert*-butoxyl radicals generated in photolysis of tertbutyl cumyl peroxide. *J. Org. Chem.* **85**, 8627–8638 (2020).
77. An, Q. et al. Cerium-catalyzed C–H functionalizations of alkanes utilizing alcohols as hydrogen atom transfer agents. *J. Am. Chem. Soc.* **142**, 6216–6226 (2020).
78. Yang, Q. et al. Photocatalytic C–H activation and the subtle role of chlorine radical complexation in reactivity. *Science* **372**, 847–852 (2021).
79. Cai, C.-Y. et al. Photoelectrochemical asymmetric catalysis enables site- and enantioselective cyanation of benzylic C–H bonds. *Nat. Catal.* **5**, 943–951 (2022).
80. Nguyen, V. T. et al. Visible-light-enabled direct decarboxylative *N*-alkylation. *Angew. Chem. Int. Ed.* **59**, 7921–7927 (2020).
81. Dang, H. T. et al. Acridine photocatalysis: insights into the mechanism and development of a dual-catalytic direct decarboxylative conjugate addition. *ACS Catal.* **10**, 11448–11457 (2020).
82. Adili, A., Korpusik, A. B., Seidel, D. & Sumerlin, B. S. Photocatalytic direct decarboxylation of carboxylic acids to derivatize or degrade polymers. *Angew. Chem. Int. Ed.* **61**, e202209085 (2022).

Acknowledgements

We are grateful for the financial support from the National Natural Science Foundation of China (22471049, W.X. and 22101066, L.G.), Science and Technology Plan of Shenzhen (JCYJ20210324133001004, W.X.; JCYJ20220531095016036, L.G.; JCYJ20230807094408017, W.X.; and GXWD20220817131550002, W.X.), Natural Science Foundation of Guangdong (2022A1515010863, L.G.), Guangdong Basic and Applied Basic Research Foundation (2021A1515220069, W.X.), Talent Recruitment Project of Guangdong (2019QN01L753, W.X.). and State Key Laboratory of Urban Water Resource and Environment (Harbin Institute of Technology) (2022TS23, W.X.). C.Z. thanks the KAUST Supercomputing Laboratory (k1284) and High Performance Computing Centers at Ningbo Institute of Digital Twin for providing the computational resources. W.X. thanks the support from the Open Research Fund of the School of Chemistry and Chemical Engineering, Henan Normal University.

Author contributions

J.Y. and L.G. conceived the concept. J.Y. performed and analyzed the experiments. C.S., A.M.H., M.L., and C.Y. contributed to the data analysis. J.Y. and L.G. wrote the manuscript. L.G. and W.X. supervised and directed the project.

Competing interests

The authors declare no competing interests.

Additional information

Supplementary information The online version contains supplementary material available at https://doi.org/10.1038/s41467-025-60429-6.

Correspondence and requests for materials should be addressed to Lin Guo or Wujiong Xia.

Peer review information *Nature Communications* thanks Hai-Chao Xu, Zhongyi Zeng, and the other, anonymous, reviewer for their contribution to the peer review of this work. A peer review file is available.